JOURNAL OF MATERIALS SCIENCE 12 (1977) 999–1009

Glass formation and phase transformations in plasma prepared Al_2O_3-SiO_2 powders

M. S. J. GANI, R. McPHERSON
Department of Materials Engineering, Monash University, Clayton, Australia

The structure of Al_2O_3–SiO_2 sub-micron powders prepared by oxidation of mixed aluminium–silicon halides in an oxygen–argon high frequency plasma flame has been studied. The powders were completely amorphous up to at least 52 wt % Al_2O_3 and partially amorphous in the range 52 to 88 wt % Al_2O_3. The crystalline phase was mullite up to 75 wt % Al_2O_3 but at higher Al_2O_3 contents a metastable solid solution of SiO_2 in γ–Al_2O_3 was observed in addition to mullite. Amorphous particles crystallized to mullite on heating to 1000° C, independently of composition. Extension of glass formation towards the high Al_2O_3 end of the Al_2O_3–SiO_2 system as the cooling rate is increased and particle size decreased, may be explained by the effect of viscosity on the nucleation rate of mullite from liquid, for Al_2O_3 contents up to 60 wt %. The viscosity change is relatively small as the Al_2O_3 content is increased beyond 60% and it is suggested that the change in nucleus–liquid interfacial energy with composition is the predominant factor controlling nucleation rate in this range. At Al_2O_3 concentrations greater than approximately 80 wt %, γ-Al_2O_3 is the phase which nucleates from the melt. A double DTA peak was observed for powders containing more than 80 wt % Al_2O_3. The lower temperature peak is believed to arise from the formation of mullite from a metastable solution of SiO_2 in γ-Al_2O_3, and the higher temperature peak from crystallization of mullite from the amorphous phase. The presence of SiO_2 in solution in metastable Al_2O_3 increases the temperature of transformation to α-Al_2O_3 to greater than 1500° C compared with 1230° C for pure Al_2O_3.

1. Introduction

Sub-micron refractory oxide powders may be prepared by condensation from the vapour phase by oxidation of a suitable volatile compound injected into an oxygen containing high-frequency plasma [1, 2]. The plasma will usually tolerate only a small concentration of reactant before extinction occurs and greater rates of production can be achieved by the injection of the reactant into the plasma tail flame [3]. In general, the oxides condense to form a mist of liquid droplets with diameters in the range 0.01 to 0.3 μm, which then subsequently solidify at temperatures considerably lower than the equilibrium freezing point. Alumina droplets crystallize as the metastable δ-Al_2O_3 modification rather than α-Al_2O_3, which is the only stable form. This may be explained by the differences in the relative nucleation energy barriers of the forms of alumina, the thermal history of the particles during cooling, and the kinetics of the transformation between the various modifications [4].

Silica particles prepared by injecting $SiCl_4$ into an oxygen plasma [3], or an oxy–hydrogen flame [5], do not crystallize and the powder produced consists of amorphous spherical particles with diameters in the range 0.01 to 0.3 μm. Al_2O_3–SiO_2 particles, 0.12 μm diameter containing 75% Al_2O_3, prepared by injecting the mixed chlorides into an oxygen–hydrogen flame have also been observed to be amorphous [6].

Several studies of the crystallization of Al_2O_3–SiO_2 melts have shown that the region of glass formation may be extended to higher Al_2O_3 concentrations as the cooling rate from the melt is increased. Glass formation has been observed to 32 mol% Al_2O_3 [7] and 40 mol% [8] using wire quench methods and to 67 mol% Al_2O_3 [8] using flame spherulization. Compositions containing up to 60 mol% Al_2O_3 could be prepared in the amorphous condition by quenching small tubes of the melt into mercury [9], or by splat-quenching melts onto water-cooled steel rollers [10]. Splat cooling has also been used to prepare glasses containing up to 75 mol% Al_2O_3 [11], and glasses containing up to approximately 80 mol% Al_2O_3 have been produced by flame spraying into water [12].

In the present study, the structure of submicron Al_2O_3–SiO_2 powders prepared by condensation from an oxygen–argon high frequency plasma flame have been examined over the complete range of compositions, in the as-prepared condition, and the phase changes which occur on subsequent heat-treatment have been investigated.

2. Experimental

Mixtures of Al_2Br_6 and $SiCl_4$ vapour were prepared by bubbling argon first through liquid $SiCl_4$ and then liquid Al_2Br_6, each held at constant temperature to control the vapour pressures and hence the proportions of the halides in the argon stream. The mixed halides were injected into the tail flame of an oxygen–argon high-frequency plasma torch and the powders formed were collected by passing the exhaust gases through an electrostatic precipitator. The apparatus has been described in detail elsewhere [13].

One of the plasma prepared powders was formed into agglomerated particles of 74 μm diameter by screening and then spheroidized by flame-spraying into water using a "Metco" oxygen-acetylene flame spraying torch.

The phases present in the powders in the as-prepared condition and after various heat-treatments, were determined by X-ray diffraction using Cu$K\alpha$ radiation in a Philips diffractometer. Powders were heat-treated in a platinum dish in a Pt–20% Rh furnace. The sample temperature was measured using a Pt/Pt–13% Rh thermocouple attached to the dish.

Transformations occurring during heat-treatment were also investigated using a Rigaku microdifferential thermal analysis apparatus. In some cases the DTA experiments were terminated at various temperatures and the samples examined by X-ray diffraction.

Powders were prepared for examination in a JEM-120 electron microscope by allowing a drop of a dispersion of the powder in an alcohol/water mixture to dry on a carbon film supported on a copper microscope grid. The particle size distribution of a powder was determined by measurement of the diameter of a minimum 1000 particles on electron micrographs using a Zeiss particle size analyser.

Flame sprayed powders were examined by optical microscopy using a Zeiss "Ultraphot" microscope. The powders were dispersed in 1-bromonapthalene which has a refractive index (1.658) similar to that of the particles examined.

3. Results

3.1. Plasma prepared powders

The particles were spherical in all powders prepared, as shown in Figs. 1 and 2. Composition, mean particle diameter and the structure of the as-prepared powders are given in Table I.

At Al_2O_3 content less than 52 wt%, the particles showed no internal structure (Fig. 1) and the electron diffraction patterns consisted only of diffuse rings, typical of an amorphous phase. At higher Al_2O_3 contents, an internal structure could be observed in some particles (Fig. 2) which also gave single crystal diffraction patterns. Some amorphous particles were observed in powders containing 88.5 wt% Al_2O_3.

The X-ray diffraction patterns for powders containing up to 52.4 wt% Al_2O_3 showed only a

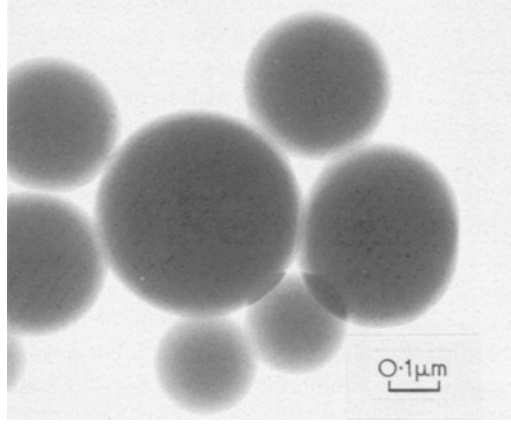

Figure 1 Al_2O_3–SiO_2 powder, 36.6 wt% Al_2O_3.

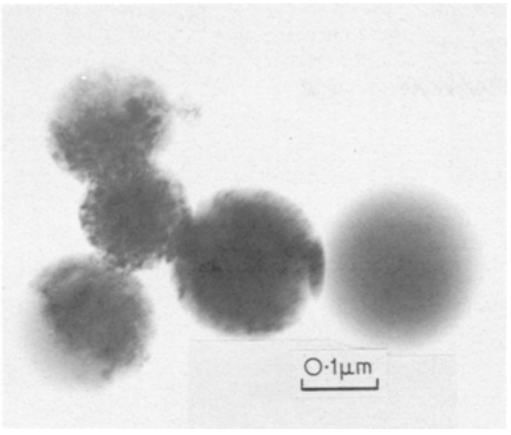

Figure 2 $Al_2O_3-SiO_2$ powder, 86.4 wt% Al_2O_3.

TABLE I Particle size and phases present for as-prepared powder

Al_2O_3 (wt%)	Mean particle diameter (μm)	Phases detected by X-ray diffraction
0	0.03	amorphous
36.6	0.22	amorphous
52.4	0.18	amorphous
57.0	0.05	amorphous + mullite
62.2	0.10	amorphous + mullite
75.0	0.18	amorphous + mullite
80.0	0.15	amorphous + mullite + γ-Al_2O_3
86.4	0.07	amorphous + mullite + γ-Al_2O_3
88.5	0.15	amorphous + mullite + γ-Al_2O_3
100	0.09	δ-Al_2O_3

broad band between 15 and 31° 2θ, typical of an amorphous structure. At higher Al_2O_3 contents, mullite lines were superimposed on the amorphous background. Both γ-Al_2O_3 and mullite lines were observed in powders containing 75 to 88.5 wt% Al_2O_3. Pure Al_2O_3 powders consisted only of δ-Al_2O_3.

The wt % mullite in the powders was determined by adding approximately 10 wt% 0.3 μm particle size α-Al_2O_3 powder (Linde A) as an internal reference and comparing the ratios of the integrated intensities of the (1 1 3) α-Al_2O_3 and (2 3 0) mullite lines with those from a series of mullite, amorphous, α-Al_2O_3 calibration mixtures. The γ-Al_2O_3 and amorphous content of powders containing >80% Al_2O_3 could not be determined quantitatively in a similar manner, because of the overlap of the strongest γ-Al_2O_3 lines with mullite and the relatively low intensity of the amorphous peak. It was possible, however, to estimate the γ-Al_2O_3 and amorphous phase content of these mixtures using information gained from DTA.

DTA curves obtained from the powders are shown in Fig. 3. The powders containing ⩽ 62.2 wt % Al_2O_3 gave single exothermic peaks and X-ray diffraction after the peaks showed that they corresponded to the crystallization of mullite. Two overlapping peaks were observed for powders with Al_2O_3 contents greater than 75 wt%. The reactions that occurred during the peaks were determined by interrupting the DTA runs at various stages, and measuring the intensities of the mullite lines and the approximate area under the amorphous peak from XRD traces (Fig. 4). The results showed that although mullite was produced by each reaction, the amount of amorphous material present decreased only during the higher temperature reaction. There was no apparent shift

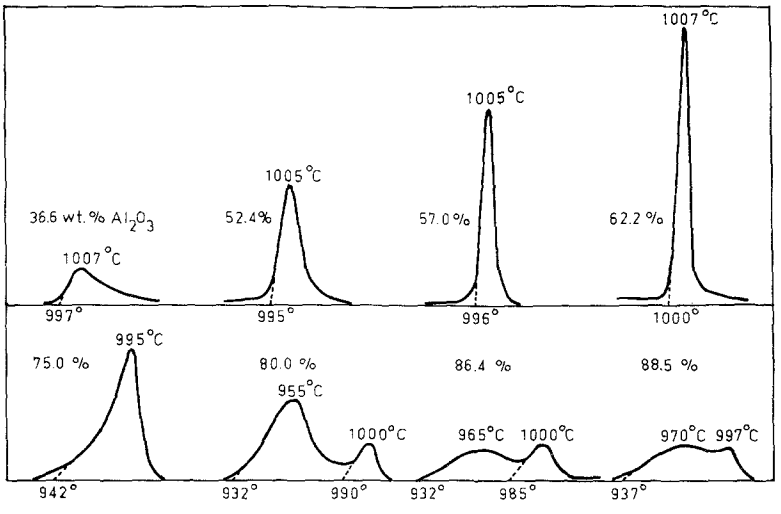

Figure 3 DTA curve for as-prepared powders as function of composition.

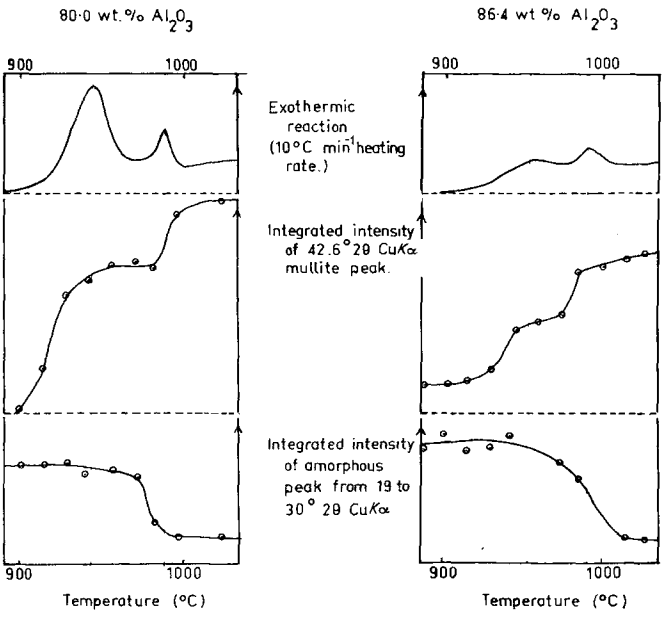

Figure 4 Changes in the intensities of mullite and amorphous phase X-ray diffraction peaks during DTA exotherms for 80.0 and 86.4 wt % Al_2O_3.

in the positions of the mullite lines during or after the reactions. It was not possible to detect any change in intensity of γ-Al_2O_3 lines because of interference from neighbouring intense mullite lines.

The wt % mullite present in the as-prepared powders was given directly from the quantitative X-ray diffraction measurements, and the wt % amorphous phase was, therefore, given by difference up to 62.2 wt % Al_2O_3. The fraction amorphous phase determined by measurement of the integrated intensities of the amorphous peak agreed closely with these values.

The area under the single DTA exotherm was assumed to be proportional to the heat of crystallization of the amorphous phase to mullite and the ratio of this peak area to the wt % amorphous phase was found to be approximately constant as expected. The experimental results (Fig. 4) show that the higher temperature exotherm, in powders containing alumina in excess of that required to form mullite, arises from crystallization of amorphous phase. The single rather broad peak observed for the 75 wt % Al_2O_3 sample was shown to consist of two overlapping peaks of approximately equal area when lower heating rates were used. The area of the second peak was consistent with crystallization of an amorphous phase constituting 63 wt % of the sample, in good agreement with the value of 66 wt % determined by measurement of the integrated intensity of the amorphous X-ray diffraction peak. Alumina could not be detected in this sample although the presence of the double DTA peak, as discussed later, suggests that some γ-Al_2O_3 was present. γ-Al_2O_3 would, however, be difficult to detect in small quantities because of interference from adjacent mullite lines; up to approximately 10% γ-Al_2O_3 by weight could be present without detection.

Since the second DTA peak appears to be associated with crystallization of the amorphous phase, the wt % amorphous phase may be estimated from the area of this peak assuming the same value for the ratio of the DTA peak area to wt % amorphous phase found for the lower Al_2O_3 powders. The wt

TABLE II Estimated wt % phases in as-prepared powders and calculated equilibrium wt %

Al_2O_3 (wt %)	Estimated wt % phases as prepared			Calculated equilibrium phases (wt %)		
	Al_2O_3	Mullite	Amorphous	SiO_2	Mullite (3:2)	Al_2O_3
0	–	–	100	100	–	–
36.6	–	–	100	49	51	–
52.4	–	–	100	27	73	–
57.0	–	1	99	21	79	–
62.2	–	10	90	13	87	–
75.0	5	31	64	–	89	11
80.0	53	19	28	–	71	29
86.4	46	21	33	–	48	52
88.5	62	3	34	–	41	59
100	100	–	–	–	–	100

% γ-Al_2O_3 present then follows by difference. The results of this treatment are shown in Table II together with the calculated wt% equilibrium phases to be expected.

The DTA curve for pure Al_2O_3 showed an exothermic peak at 1230° C corresponding to the transformation of δ-Al_2O_3 to α-Al_2O_3; this was not observed, however, for metastable alumina containing SiO_2. It was found that γ-Al_2O_3 was present after the formation of mullite in powder containing 80 wt% Al_2O_3. The γ-Al_2O_3 transformed to δ-Al_2O_3 at approximately 1100° C and the δ-Al_2O_3 to θ-Al_2O_3 transformation occurred between 1170 and 1430° C. No α-Al_2O_3 formation was observed up to the maximum operating temperature of 1500° C for the DTA apparatus used. Heat-treatment for 1 h at 1400° C resulted in a mixture of mullite and θ-Al_2O_3 in samples containing 80 wt% Al_2O_3; α-Al_2O_3 could be formed by heating the powders for 1 h at 1500° C.

Crystallization of the amorphous material remaining after the formation of mullite in the 62.2 wt% Al_2O_3, powder was not observed up to the 1500° C limit of the DTA apparatus. However, some cristobalite was formed after heating for 1 h at 1400° C.

Endothermic inflections observed in the DTA curve of powders containing 36.6, 52.4, 57.0 and 62.2 wt% Al_2O_3 at 925, 935, 945 and 962° C respectively, that is before crystallization of mullite, were assumed to be the glass transition temperatures (T_g). The ratio of T_g to the liquidus temperature (T_m) was 0.56 to 0.58, which is in good agreement with published data for SiO_2–10 wt% Al_2O_3 glass [14].

X-ray diffraction of the as-prepared flame spheroidized particles containing 86.4 wt% Al_2O_3 showed that they consisted of mullite, γ-Al_2O_3 and glass. Optical microscopy revealed that some of the particles, particularly the larger ones, had completely crystallized to one or a few crystals, the remainder were amorphous. DTA traces of the powder gave a single sharp exothermic peak with a maximum at 1000° C. Microscopic examination of powders heated to above 1000° C showed that the previously amorphous particles had crystallized to a fine polycrystalline structure and X-ray diffraction confirmed that the DTA peak was associated with crystallization of the amorphous particles to mullite.

4. Discussion

4.1. Condensation of particles

The uniformity of composition of the particles within a sample is of considerable importance when considering the structure of mixed oxide powders condensed from the vapour phase. It has been shown that the major factor controlling particle growth in the formation of SiO_2 from flames is coalescence of particles on collision over the temperature range in which the particles are liquid. That is, between the temperature at which condensation is complete and the temperature at which condensation is complete and the temperature at which the particles effectively solidify [15]. An examination of the partial pressures of species in equilibrium with liquid solutions suggests that virtually all of the Al_2O_3 and SiO_2 will condense to liquid droplets at temperatures well above their effective freezing points and the final particles will be formed as a result of the coalescence of several thousand "nuclei" [16]. The combined effects of reaction at particle surfaces to give co-condensation of both species into the initial droplets, together with mixing by coalescence of many small droplets would be expected to result in all the particles within a powder having a composition very close to the average composition of the powder provided that the proportions of Al and Si in the vapour remained constant. In practice, changes in the temperatures of the halide baths during an experimental run would produce variations in the composition from particle to particle. The range of variation from this cause was estimated to be no greater than ± 5% under the conditions employed in the present work.

4.2. Glass formation

The observations of glass formation to quite high Al_2O_3 contents in the present work is consistent with previous studies in which rapid cooling from the melt has been employed [7, 11]. Crystallization must be suppressed for a glass to be formed. This means that either the nucleation rate as a function of temperature is such that there is a low probability of nucleus formation in the volume of liquid under consideration within the time available during cooling, or that the crystal growth rate is so low that negligible growth occurs if nucleation does take place.

Homogeneous nucleation of crystallization would be expected during the formation of

powders by the plasma technique in which small droplets condense from the vapour at high temperature and each droplet cools in isolation [4]. In silicate systems it is usually considered that glass formation is a result of the large activation energy for rearrangement of the molecules which is manifested as high viscosity near the melting point. Turnbull has suggested the following simplified equation for homogeneous nucleation from the melt in systems where viscosity is significant [17]

$$I = \frac{k_n}{\eta} \exp\left[-b\alpha^3\beta/T_r(\Delta T_r)^2\right] \quad (1)$$

where k_n = a constant, η = viscosity, b = nucleus shape factor = $16\pi/3$ for spherical nucleus, T_r = reduced temperature = T/T_m, ΔT_r = reduced undercooling = $(T_m - T)/T_m$, T_m = equilibrium melting point, and α and β are dimensionless parameters given by

$$\alpha = \frac{(N\bar{V}^3)^{1/3}\sigma}{\Delta H_m} \quad (2)$$

$$\beta = \frac{\Delta H_m}{RT_m} \quad (3)$$

where N = Avogadro's number, $\bar{V}$ = molar volume, σ = liquid–solid interfacial energy, ΔH_m = molar heat of fusion, R = gas constant. The effect of viscosity on nucleation rate may, therefore, be estimated using measured viscosity–temperature data.

The nucleation rate as a function of T_r was estimated in this way as a function of composition for the Al_2O_3–SiO_2 system. Published viscosity data [18, 19] were extrapolated to temperatures below T_m using the Fulcher equation [20]

$$\eta = A \exp\left(\frac{B}{T - T_0}\right) \quad (4)$$

where A and B are constants and T_0 is a characteristic temperature which was taken as the glass transition temperature (T_g); the observed value of $T_g = 0.57T_m$ was used. The factor $\alpha\beta^{1/3}$ was assumed constant at 0.5, a value commonly found for inorganic systems [17]. There is considerable uncertainty in the value of k_n to be used; the calculated value of k_n/η is 10^{35} cm^{-3} sec^{-1} for metals, where $\eta \simeq 10^{-2}$ P at T_m, giving $k_n = 10^{33}$ dyn cm, however the experimental value of k_n/η is $10^{42\pm2}$ [18]. The large difference has been explained in terms of the assumptions made when the theory was applied to the nucleation of crystallization in mercury droplets [21]. In practice, the large range of values quoted for the pre-exponential term of the nucleation equation is not significant when dealing with the effective nucleation temperature of a system because of the very large change in the exponential term with small changes in temperature. It becomes more important, however, when attempts are made to calculate nucleation rates. The effect of changes in k_n is to translate nucleation rate-reduced temperature curves as a whole along the nucleation rate axis. In subsequent discussion, the value of $k_n = 10^{38}$ is used, that is the experimental value, because this gives nucleation rates which are consistent with the observation that liquid Al_2O_3 droplets crystallize even at the most extreme cooling rates yet employed.

The nucleation rate calculated in this way, as a function of T_r, is shown in Fig. 5 for 0, 20, 30, 60 and 100% Al_2O_3. As expected this shows extremely low nucleation rates for pure SiO_2 and increasing nucleation rates with increasing Al_2O_3 content. Crystallization will occur if the number of nuclei per particle (n) is greater than 1 during the cooling period where n is given by

$$n = v\int_0^t I\,dt \quad (5)$$

where v = particle volume and t = time.

For plasma prepared powders, $v \simeq 10^{-16}$ cm^3 and the cooling rate $\simeq 10^{4\circ}$ C sec^{-1} [4]. Using this data in Equation 5 together with the maximum nucleation rate from Fig. 5 suggests that glass formation could be expected up to approximately 50 wt % Al_2O_3 but not beyond, if glass formation

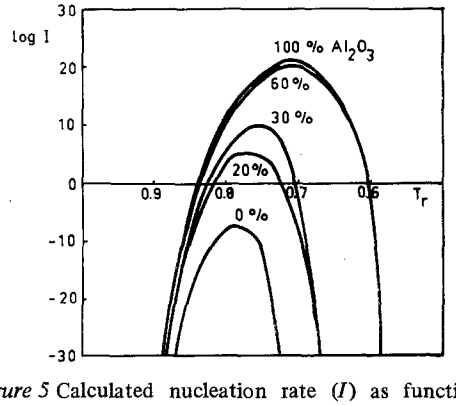

Figure 5 Calculated nucleation rate (I) as function of reduced temperature (T_r) and composition.

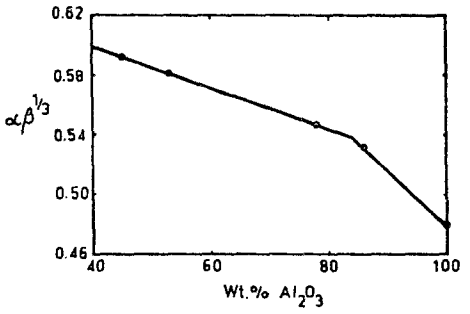

Figure 6 $\alpha\beta^{1/3}$ as function of composition estimated from published data.

is a function of viscosity only. There is very little difference between the nucleation rate curves for pure Al_2O_3 and SiO_2–60 wt% Al_2O_3 suggesting that the observed extension of glass formation to 80 wt% Al_2O_3 arises from a change in $\alpha\beta^{1/3}$ with composition. Since the viscosity effect is apparently small in the range 60 to 100 wt% Al_2O_3 an estimate of $\alpha\beta^{1/3}$ may be made from observed limits of glass formation over this composition range as a function of specimen volume, cooling rate and composition. The nucleation rate required to give crystallization at the limiting Al_2O_3 content for glass formation reported in several published studies [7, 8, 12], was calculated from the estimated cooling rate and sample volume for each of the methods used. The data and nucleation rates are summarized in Table III. The nucleation rate was then substituted in Equation 1 to give the estimated variation of $\alpha\beta^{1/3}$ with composition shown in Fig. 6. The value used for 100% Al_2O_3 is that estimated for nucleation of γ-Al_2O_3 [4]. It is tempting to suggest that the curve consists of two segments, one for 80 to 100% Al_2O_3 corresponding to the formation of a metastable Al_2O_3 nucleus and the other for $Al_2O_3 < 80$ wt% for formation of a mullite nucleus. Although the data are not sufficiently reliable for such a conclusion to be drawn, a change in nucleation behaviour of this sort clearly must occur between pure Al_2O_3 and the mullite composition depending upon the variation of the free energy difference between the possible nucleus phases and the liquid, and the interfacial energy between nucleus phases and liquid.

Nucleation rates as a function of T_r and composition calculated using the variation of viscosity with temperature and composition and the estimated values of $\alpha\beta^{1/3}$ are shown in Fig. 7. The number of nuclei per particle (n) formed during cooling, is plotted as a function of Al_2O_3 content, particle size and cooling rate in Fig. 8. Application of these results to the plasma prepared powders predicts glass formation to 85 wt% Al_2O_3 for a cooling rate of 10^4 °C sec^{-1} and 0.1 μm particle diameter. In practice the particle size ranges from 0.01 to 0.3 μm giving the curve shown in Fig. 9 for fraction crystalline as a function of Al_2O_3 concentration; the experimentally observed points are also shown. There is reasonable agreement between the observed and calculated fraction crystalline considering the uncertainty in both the estimated values of the fraction amorphous phase and the range of composition of particles within a powder. The more serious of these is the variation of composition from particle to particle which will tend to

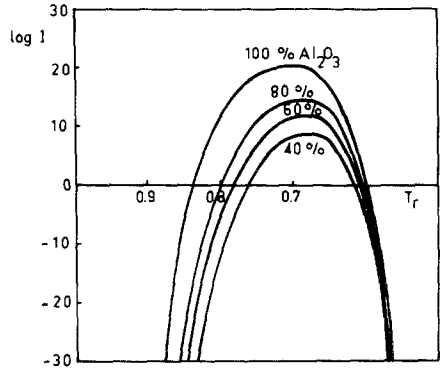

Figure 7 Calculated nucleation rate (I) as function of reduced temperature (T_r) and composition taking into account variation of $\alpha\beta^{1/3}$ with composition.

TABLE III Data for glass formation limits in SiO_2–Al_2O_3

Method used	Reference	Limiting Al_2O_3 content (wt%)	Estimated cooling rate (° C sec^{-1})	Sample volume (cm^3)	I (cm^{-3} sec^{-1})
Wire quench	[7]	45	10^3	10^{-3}	2×10^3
Wire quench	[8]	53	5×10^3	3.4×10^{-5}	1.3×10^5
Flame spherulization	[8]	78	10^5	1.4×10^{-8}	1.4×10^{10}
Flame spherulization	[12]	86	10^7	1.4×10^{-8}	1.4×10^{12}

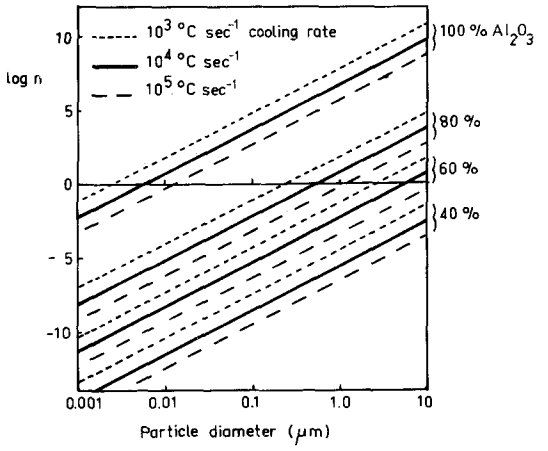

Figure 8 Calculated number of nuclei per particle as a function of particle diameter, cooling rate and composition.

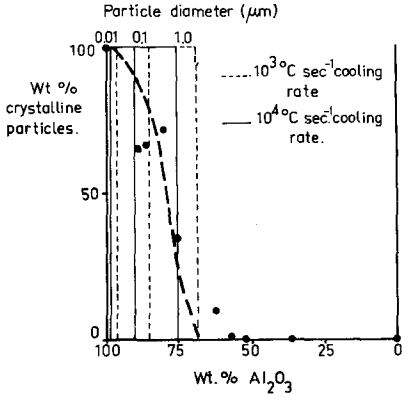

Figure 9 Estimated wt % crystalline as function of composition. Experimental points shown.

spread the apparent composition range over which the transition from glass to crystalline structure occurs.

The above analysis indicates that the reduction in viscosity of the melt with increasing Al_2O_3 content can explain the extension of the composition range in which glass is formed as the cooling rate is increased and/or the sample size decreased, up to 60 wt % Al_2O_3. Beyond this level the change in the viscosity effect is small and crystallization apparently occurs in compositions with higher Al_2O_3 contents because of a reduction in the parameter $\alpha\beta^{1/3}$ as the Al_2O_3 concentration is increased towards 100%. The major variable contributing to $\alpha\beta^{1/3}$ is the liquid–solid interfacial energy which is, in general, unknown. The interfacial energy between liquid Al_2O_3 and γ-Al_2O_3 is probably relatively low [4] and increases as the proportion of SiO_2 in solution in the liquid phase is increased until a composition is reached at which $\alpha\beta^{1/3}$ is the same for nucleation of both mullite and γ-Al_2O_3; at higher SiO_2 contents, mullite would nucleate rather than Al_2O_3. It is this change of $\alpha\beta^{1/3}$, therefore, which controls the nucleation kinetics between 60 and 100 wt % Al_2O_3, and hence the composition limit at which a glass is formed under specified cooling conditions. It is unlikely that differences in crystal growth rate are significant in glass formation at high Al_2O_3 concentrations because growth rate at viscosities greater than 1 *P* is inversely proportional to viscosity [17]. There would, therefore, be little difference in growth rate over the composition range 60 to 100 wt % Al_2O_3.

4.3. Transformation of powders on heat-treatment

The results show that the single exothermic reaction observed by DTA for the alumina–silica powders containing less than 63 wt % Al_2O_3 results from the crystallization of mullite from the originally amorphous material. Powders containing more than 75 wt % Al_2O_3, however, gave double exothermic peaks, during both of which mullite was formed. The amount of amorphous material decreased only during the second exothermic reaction which indicates that the mullite formed during this reaction originated from the amorphous particles in the powder. This may be compared with the results of Takamori and Roy [12] who observed a single exotherm associated with the crystallization of Al_2O_3–SiO_2 glasses over the complete composition range examined (i.e. 10 to

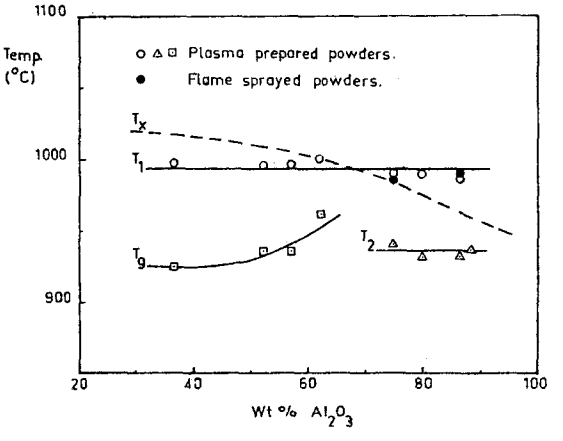

Figure 10 DTA peak temperatures as function of composition. T_1 crystallization of amorphous phase, T_2 formation of mullite from γ-Al_2O_3/SiO_2, T_g glass transition temperature, T_x results of Takamori and Roy [12].

90 wt % Al_2O_3). The temperatures of the DTA peaks observed in the present work are compared with those of Takamori and Roy in Fig. 10. The same criterion for reaction temperature was used, that is, the extrapolated onset of the peak. The temperatures agree reasonably well up to 70 wt % Al_2O_3 although the present work is consistent with a constant temperature of crystallization of 990° C whereas Takamori and Roy observed a decrease in temperature with increasing Al_2O_3 content. The DTA curve for the flame spheroidized powder containing 86.7 wt % Al_2O_3 gave a single, sharp exothermic peak at 990° C indicating that the double peak observed in the plasma prepared powders is a function of their structure which differs from the larger flame spheroidized particles investigated by Takamori and Roy. The observations that the second DTA peak appears to be associated with crystallization of amorphous particles, and that the intensity of the mullite X-ray diffraction lines increase during the first peak suggest that the first peak is associated with formation of mullite from a metastable crystalline phase. The fact that the ratio of alumina to mullite in the as-prepared powder is considerably greater than the calculated equilibrium values (Table II) suggests that the γ-Al_2O_3 phase formed during cooling of the particles contains SiO_2 in solid solution. The first DTA peak could, therefore, arise from crystallization of mullite from this metastable solution.

The formation of a metastable γ-Al_2O_3 phase containing SiO_2 in solution, that is a silicon–aluminium defect spinel, has been postulated as an intermediate stage in the crystallization of mullite from meta-kaolinite. This is supported by careful lattice parameter measurements although there is no direct evidence for the composition of the phase [22].

The structure of particles as revealed by electron microscopy suggests that they are either completely amorphous or completely crystalline. This would be expected if crystallization is nucleation controlled as discussed previously. The analysis of nucleation of crystallization of the droplets also suggests that there is a change in the phase nucleated from mullite to γ-Al_2O_3 at approximately 80 wt % Al_2O_3.

The amount of mullite ($3Al_2O_3 \cdot 2SiO_2$) formed from a γ-Al_2O_3/SiO_2 solid solution, calculated from the estimated phase constitution and chemical composition of the as-prepared powders (Table II) is given in Table IV.

The ratio of the area of the first DTA peak to the wt % mullite which could be formed by decomposition of the γ-Al_2O_3/SiO_2 phase (third column, Table IV) is approximately constant for the powders containing 80.0, 86.4 and 88.5 wt % Al_2O_3. A reliable value for the ratio could not be determined for the 75 wt % Al_2O_3 powder because of uncertainty in the amount of γ-Al_2O_3 present, and overlap of the DTA peaks.

The ratios of the increase of intensity of the mullite XRD lines after the first and second DTA peaks (fourth column, Table IV) are in good agreement with the ratios of the amounts of mullite formed as calculated from the phase constitution and composition (fifth column, Table IV).

The results are, therefore, consistent with the hypothesis that the first DTA peak is associated with crystallization of mullite from a metastable solution of SiO_2 in γ-Al_2O_3 and the second peak arises from crystallization of mullite from the amorphous phase.

The fact that only single exotherms are obtained on heat-treatment of γ-Al_2O_3/SiO_2 particles tens of microns diameter, prepared by quenching liquid melts containing Al_2O_3 in excess of that required to form mullite, may be interpreted if the effect of the heat of fusion release on crystallization is taken into account. It has been shown for flame and plasma prepared alumina powder that the increase in temperature of an under-cooled liquid droplet on solidification is strongly dependent upon particle diameter [4]. For sub-micron particles the heat of fusion is dissipated at about the

TABLE IV

Al_2O_3 (wt %)	wt % mullite from γ-Al_2O_3/SiO_3	Ratio area 1st DTA peak to wt % mullite formed	Ratio increase in intensity mullite XRD line after 1st and 2nd DTA peaks	Ratio calculated mullite formed during 1st and 2nd DTA peaks
80.0	38	1.3	1.1	0.9
86.4	23	1.1	2.1	1.8
88.5	25	1.0	–	–

same rate as it is released; however, for particles larger than approximately 10 μm diameter, the rate of removal of heat is such that the particle temperature increases by several hundred degrees. This results in transformation, to the equilibrium phase, of the metastable nucleus which formed because of a lower energy barrier to nucleation.

Similarly those sub-micron Al_2O_3–SiO_2 particles containing more than approximately 80 wt % Al_2O_3 which crystallize on cooling would tend to retain the nucleus structure, i.e. a metastable solution of SiO_2 in γ-Al_2O_3. However, for particles tens of microns diameter, the temperature rise produced by the release of the heat of fusion could be such that the nucleating phase transforms to the equilibrium structure of mullite plus alumina.

In sub-micron particles, therefore, the metastable solution of SiO_2 in γ-Al_2O_3 is preserved to room temperature and gives rise to the first DTA peak, whereas in flame spheroidized powders the γ-Al_2O_3/SiO_2 which nucleates transforms to mullite during cooling and the DTA peak observed arises only from crystallization of amorphous particles. The observation that the particles of the flame spheroidized powder were either completely amorphous or consisted of one or a few crystals of mullite is consistent with rapid crystallization of the first one or two nuclei formed in a particle and supports the above hypothesis.

The observed increase of transformation temperature of the metastable alumina remaining after mullite crystallization must be associated with residual SiO_2 remaining in solution.

The influence of silica on the transformation temperatures of the metastable forms of alumina has been noted by Iler [23] who found that the addition of silicic acid to fibrillar colloidal boehmite retarded the conversion of γ-Al_2O_3 to θ-Al_2O_3 and α-Al_2O_3. Additions of 20% SiO_2 stabilized γ-Al_2O_3 to 1150° C, θ-Al_2O_3 was only observed in samples heated at 1150° C for 24 h and κ-Al_2O_3 and α-Al_2O_3 appeared in samples heated for 25 h at 1200° C. More recently, Yoldas [24] has reported the stabilization of metastable alumina in Al_2O_3–SiO_2 powders prepared by pyrolysis of sols. The maximum effect was observed for 6 wt % SiO_2 at which the temperature of transformation to α-Al_2O_3 was 1380° C compared with 1200° C for pure Al_2O_3.

In the absence of SiO_2, δ-Al_2O_3 is the phase isolated in plasma prepared powders and it has been suggested that although γ-Al_2O_3 is probably the phase which nucleates, the cooling rate is sufficiently low to permit the re-arrangement of γ-Al_2O_3 to the more ordered δ-Al_2O_3 during cooling [4]. Heat-treatment of pure δ-Al_2O_3 results in direct transformation to α-Al_2O_3 at 1230° C with negligible θ-Al_2O_3 formation. The presence of SiO_2 in the γ-Al_2O_3 structure apparently sufficiently decreases the rate of transformation to other forms to prevent the formation of δ-Al_2O_3 during cooling of plasma prepared sub-micron Al_2O_3–SiO_2 powders. The γ-Al_2O_3/SiO_2 transforms to δ-Al_2O_3 on heat-treatment at 1100° C and, in turn, transforms to θ-Al_2O_3 in the range 1170 to 1430° C (at 20° C min^{-1} heating rate). α-alumina is only formed at temperatures greater than 1500° C, considerably higher than the temperatures observed for SiO_2-doped Al_2O_3 prepared by precipitation methods [23, 24].

The effect of SiO_2 on the temperature of the transformation of metastable alumina to α-Al_2O_3 must arise from an increase in the activation energy for the process. This could be produced either by an increase in the stability of the metastable form, i.e. a decrease in its free energy relative to α-Al_2O_3; or by a direct increase in the energy barrier, that is, an increase in energy of the configurations through which the structure must pass during transformation. However, the free energy difference between γ-Al_2O_3 and α-Al_2O_3 is relatively small at elevated temperatures, 2.5 kcal mol^{-1} at 1500 K [25], compared with the activation energy of the transformation of γ-Al_2O_3 to α-Al_2O_3, 116 kcal mol^{-1} [26]. Since γ-Al_2O_3 containing SiO_2 in solution transforms slowly (via θ-Al_2O_3) to α-Al_2O_3 at 1250° C, the structure remains metastable with respect to α-Al_2O_3 and, therefore, the effect of SiO_2 on the transformation must be by a direct increase in the activation energy of the process.

Silicon ions incorporated into the metastable aluminas would be expected to be strongly bound within tetrahedral sites of the distorted face centred cubic packing of oxygen ions and, since transformation to α-Al_2O_3 requires rearrangement of the oxygen ions to close packed hexagonal packing, the strong, directed, silicon–oxygen bonds would have to be broken and reformed. This could explain the high activation energy observed for transformation to α-Al_2O_3, that is, the silicon ions tend to "lock" the metastable structure at high

temperatures by preventing rearrangement of the oxygen ions. The presence of SiO_2 would, on the other hand, be expected to have a relatively small effect on the transformations, γ-Al_2O_3 to δ-Al_2O_3 to θ-Al_2O_3 which require only rearrangement of the Al ions within basically the same oxygen ion lattice. This is supported by the present study in which transformation of γ-Al_2O_3 to δ-Al_2O_3 was followed by transformation to θ-Al_2O_3 in SiO_2-containing powders whereas the latter process is overshadowed in pure Al_2O_3 by the transformation of δ-Al_2O_3 directly to α-Al_2O_3.

5. Conclusions

Glass formation in sub-micron Al_2O_3–SiO_2 powders condensed from a plasma may be explained in terms of the high activation energy for atomic rearrangement in the liquid phase in the range 0 to 60 wt% Al_2O_3. At higher Al_2O_3 contents, the nucleation rate of mullite (60 to 80 wt% Al_2O_3) and γ-Al_2O_3 (80 to 100 wt% Al_2O_3) appears to be controlled by changes in liquid–crystal interfacial energy with composition.

The temperatures of crystallization of mullite from the amorphous Al_2O_3–SiO_2 phase is 990° C, which is independent of composition.

The metastable γ-Al_2O_3/SiO_2 phase nucleated at high Al_2O_3 concentrations is retained to room temperature in sub-micron powders but is not observed in flame spheroidized powders. This is because the release of the heat of fusion during crystallization of large ($\simeq 30\,\mu m$) particles produces an increase in temperature for a sufficient time to cause transformation of the nucleus phase to the stable phase in large particles but not in sub-micron particles.

A double DTA peak observed for high Al_2O_3 powders may be explained by crystallization of mullite from the metastable γ-Al_2O_3/SiO_2 phase at the lower temperature and the amorphous phase at the higher temperature.

The presence of SiO_2 in γ-Al_2O_3 results in an increase in the temperature of transformation to α-Al_2O_3 by $\simeq 300°$ C but has relatively little effect on the γ-Al_2O_3 to δ-Al_2O_3 to θ-Al_2O_3 temperatures. It is suggested that SiO_2 increases the activation energy for the transformation of metastable Al_2O_3 to α-Al_2O_3 because of the high energy required to break silicon–oxygen bonds necesssary to allow rearrangement of the oxygen ions.

Acknowledgement

M. S. J. Gani held a Commonwealth Post-graduate Research Award during the period in which this work was carried out.

References

1. T. I. BARRY, R. K. BAYLISS and L. A. LAY, *J. Mater. Sci.* 3 (1968) 229.
2. *Idem, ibid* 3 (1968) 239.
3. A. AUDSLEY and R. K. BAYLISS, *J. Appl. Chem.* 19 (1969) 33.
4. R. McPHERSON, *J. Mater. Sci.* 8 (1973) 851.
5. R. CAILLAT, J. P. CUER, J. ELSTON, F. JUILLET, R. POINTUD, M. PRETTRE and S. J. TEICHNER, *Bull. Soc. Chim. Fr.* (1959) 152.
6. J. P. CUER, J. ELSTON and S. J. TEICHNER, *ibid* (1961) 89.
7. M. S. R. HAYNES and H. RAWSON, Phys. Chem. Glasses 2 (1961) 1.
8. D. J. THORNE, *Proc. Brit. Ceram. Soc.* 14 (1969) 131.
9. S. ARAMAKI and R. ROY, *J. Amer. Ceram. Soc.* 45 (1962) 229.
10. J. F. MacDOWELL and G. H. BEALL, *ibid* 52 (1969) 17.
11. P. T. SARGEANT and R. ROY, in "Reactivity of Solids", edited by J. R. Mitchell, R. C. de Vries, R. W. Roberts and P. Cannon (Wiley, New York, 1969) p. 725.
12. T. TAKAMORI and R. ROY, *J. Amer. Ceram. Soc.* 56 (1973) 639.
13. M. S. J. GANI and R. McPHERSON, *J. Aust. Ceram. Soc.* 8 (1972) 65.
14. K. NASSAU, J. W. SHIEVER and J. T. KRAUSE, *J. Amer. Ceram. Soc.* 58 (1975) 461.
15. R. W. HERMSEN and R. DUNLAP, *Combustion and Flame* 13 (1969) 253.
16. R. McPHERSON, Proceedings of the International Round Table on Study and Application of Transport Phenomena in Thermal Plasmas, edited by C. Bonet (IUPAC/CNRS, Odeillo, 1975).
17. D. TURNBULL, *Contemp. Phys.* 10 (1969) 473.
18. V. P. ELYUTIN, V. I. KOSTIKOV, B. S. MITIN and Yu A. NAGIBIN, *Russ. J. Phys. Chem.* 43 (1969) 316.
19. R. ROSSIN, J. BERSAN and G. URBAIN, *Compt. Rend. Hebd. Seance Acad. Sci. Paris* 258 (1964) 562.
20. G. S. FULCHER, *J. Amer. Ceram. Soc.* 8 (1925) 339.
21. D. TURNBULL, *J. Chem. Phys.* 20 (1952) 411.
22. G. W. BRINDLEY and M. NAKAHIRA, *J. Amer. Ceram. Soc.* 42 (1959) 319.
23. R. K. ILER, *ibid* 47 (1964) 339.
24. B. E. YOLDAS, *J. Mater. Sci.* 11 (1976) 465.
25. D. R. STULL and H. PROPHET, JANAF Thermochemical Tables, 2nd Edn. (1971) NSRDS-NBS37.
26. C. J.-P. STEINER, D. P. H. HASSELMAN and R. M. SPRIGGS, *J. Amer. Ceram. Soc.* 54 (1971) 412.

Received 24 May and accepted 20 October 1976.